Journal of
Mechanical
Science and
Technology

Journal of Mechanical Science and Technology 21 (2007) 2048~2058

# Robust force control of a hybrid actuator using quantitative feedback theory

Kyoung Kwan Ahn*, Nguyen Huynh Thai Chau and Dinh Quang Truong

*School of Mechanical and Automotive Engineering, University of Ulsan, Korea*

(Manuscript Received April 13, 2006; Revised June 28, 2007; Accepted July 7, 2007)

**Abstract**

The use of hydraulic systems in industrial applications has become widespread due to their advantages in efficiency. In recent years, hybrid actuation systems, which combine electric and hydraulic technology into a compact unit, have been adapted to a wide variety of force, speed and torque requirements. A hybrid actuation system resolves energy consumption and noise problems characteristic of conventional hydraulic systems. A new, low-cost hybrid actuator using a DC motor is considered to be a novel linear actuator with various applications such as robotics, automation, plastic injection-molding, and metal forming technology. However, this efficiency gain is often accompanied by a degradation of system stability and control problems. In this paper, to satisfy robust performance requirements, tracking performance specifications, and disturbance attenuation requirements, the dèsign of a robust force controller for a new hybrid actuator using Quantitative Feedback Theory (QFT) is presented. A family of plant models is obtained from measuring frequency responses of the system in the presence of significant uncertainty. Experimental results show that the hybrid actuator can achieve highly robust force tracking even when environmental stiffness set-point force varies. In addition, it is understood that the new system reduces energy use, even though its response is similar to that of a valve-controlled system.

*Keywords*: Quantitative feedback Theory (QFT); Robust control; Nonlinear systems; Force control; Hybrid actuator; Hydraulic.

## 1. Introduction

Hydraulic systems play an important role in industrial mechanics. Hydraulic technology has been developed rapidly to enhance performance parameters such as accurate speed control, high power-weight ratios, physical size, controllability, reliability, cost, and so on. Recently, energy consumption and noise level have become important factors in evaluating the performance of hydraulic equipment. Most previous hydraulic actuators, however, were controlled completely by a valve; a large mount of energy is lost to heat in this process due to throttle losses at the control valves. These models are difficult to use in mobile machines because of the complication of components. To overcome these limitations of a conventional system and to satisfy new requirements, a new kind of hydraulic actuator called a hybrid actuator is proposed.

The hybrid actuator is known as a powershift system, which shifts from the high-speed electric to high-force hydraulic, creating a sleeker, cleaner and more energy-efficient way to produce large amounts of force. These energy saving features of the hybrid actuator were proven clearly by Rahmfeld and his colleague [1]. The authors developed a precise mathematical model describing energy losses in a hybrid actuator including servo pump losses, cylinder losses, and pressure losses in hydraulic lines. In addition, the paper included a comparison between the uses of a conventional hydraulic actuator and a hybrid actuator in the load-sensing system. Because of its advantages, a hybrid actuator has a wide range of applications, such as in plastic injection-molding, metal forming

*Corresponding author. Tel.: +82 52 259 2282, Fax.: +82 52 259 1680
E-mail address: kkahn@ulsan.ac.kr

metal forming technology, and aeronautics [2]. It is also highly suitable for end-effector joints, especially in robotics technology, where force or pressure control is necessary. Hence, a method for achieving force control with a new, low cost hybrid actuator is presented in this paper. With features peculiar to hydraulics, a hybrid actuator is considered to be a novel linear actuator that has many applications, due to its light weight, small size, and lack of piping, because the electronic motor (DC motor) and hydraulic components (pump, valve and cylinder) are unified. Despite its simple design, control of hybrid actuator is very complex, due to its nonlinearity, oscillatory motion, time-dependent properties, and difficulties of analytical modeling. Apart from the nonlinearities, large uncertainties exist in hydraulic systems because of the instability of some hydraulic parameters such as bulk modulus, the compressibility of oil, and changes in the environmental stiffness [3].

In the literature, to overcome these difficulties, several force control strategies have been proposed for conventional hydraulic systems. Alleyne et al. [4] showed that a conventional PID controller does not yield reasonable performance over a wide range of operating conditions. Chen et al. [5] designed a variable-structure force controller for a single-rod hydraulic cylinder. Using position, velocity, acceleration, force, and pressure feedback signals, the variable-structure controller proved to be capable of handling both static and dynamic force control tasks. The controller, however, showed steady state errors for step inputs, and the control signal was discontinuous. Wu et al. [6] implemented a generalized predictive force control algorithm for a hydraulic actuator. The controller was experimentally evaluated with respect to various types of environmental stiffness. The method, however, relies heavily on on-line parameter estimation and consequently demands a large computational time. Conrad and Jensen [7] used combinations of velocity feed-forward, output feedback, and a Luenberger observer with state estimate feedback for force control of a double-rod hydraulic actuator. However, load variations were not considered in their study. Despite the existence of a great number of force control concepts, methods, and algorithms applied to conventional hydraulic actuators, the hybrid actuator is a new concept and there is little research on its force control. As results, Grabbel [8] presented two different control strategies for controlling the position and velocity of a hybrid actuator, and succeeded in overcoming the low damping ratio problem, but the strategies performed poorly when loads varied. To illustrate the tradeoffs of hydraulic servo systems and hybrid systems, Andersson and his colleagues [9-11] used a multi-objective genetic algorithm to optimize these systems and elucidate the advantages of different concepts based on optimization results and sensitive analysis.

The objective of this paper is to present the design of a robust force controller for the new hybrid actuator using Quantitative Feedback Theory (QFT) technique. The controller is designed to satisfy robust performance requirements, tracking performance specifications, and disturbance attenuation requirements. The QFT technique has been successfully applied to solve many engineering problems, including robot position control [12], flight control actuators [13] and manufacturing systems [14]. In controlling conventional hydraulic actuators, Niksefat et al. [15] succeeded in using a nonlinear QFT technique to design a robust force controller, which can overcome many of nonlinear and uncertain characteristics of experimental industrial hydraulic actuators. The nonlinear plant is equivalently replaced by a family of linear, time-invariant transfer functions synthesized using offline measurement of inputs and outputs over a wide range of operating conditions. To improve the performance of a variable-displacement hydraulic vane pump, Thompson et al. [16] developed and optimized a robust controller via the QFT technique. The simulation results showed that the closed-loop system response remained stable under variation of fluid bulk modulus and linkage area parameters. This paper proposes a new application of the QFT technique to a hybrid actuator design. In this approach, a family of linear time-invariant transfer functions for a hybrid actuator is obtained from experimental frequency responses of the system in the presence of significant uncertainty. From the various stiffness and set-point forces, experimental results show that the new hybrid actuator could achieve highly robust force tracking.

The rest of this paper is organized as follows: In section 2, the model of the new energy-saving and low noise hybrid actuator used in this study is described. Section 3 is a comparison of the proposed system with a conventional hydraulic system. In section 4, the procedure of designing a robust force controller is described, and section 5 shows the experimental results. Finally, some conclusions are made in section 6.

## 2. Experimental setup

### *2.1 Experimental apparatus*

The schematic diagram of the new hybrid actuator is shown in Fig. 1. To generate a flow demand, the speed of a DC motor is controlled by the pulse width modulation (PWM) principle through a driver circuit using IGBTs (SGH80N60UF). The system hardware consists of an IBM-compatible personal computer (Pentium 1GHz), which is used to get the feedback signal through an A/D board (Advantech, PCI 1711) and calculates PWM to control input signals. The contact force is measured by a load cell (SETech, YC 60-500K). Springs with various stiffnesses (from 30 to 75 KN/m) are used to simulate the contact environments. A photograph of the experimental apparatus is shown in Fig. 2.

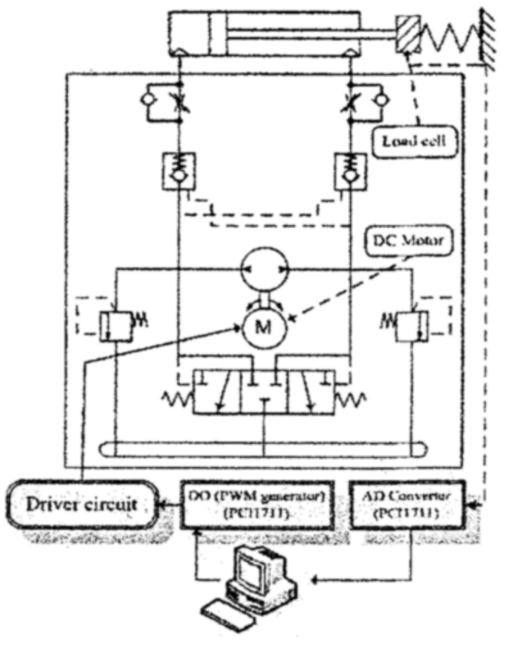


Fig. 1. Schematic diagram of a hybrid actuator.

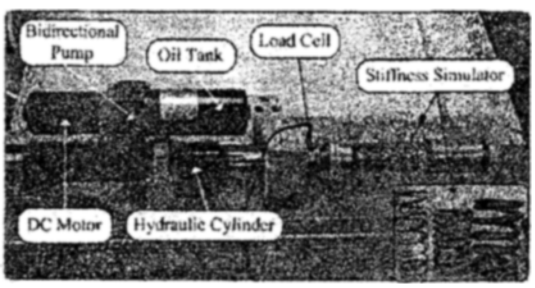


Fig. 2. Photograph of the experimental apparatus.

### *2.2 Characteristics of MMP*

In the field of fluid power control, the driving concept using a hydraulic pump with variable rotational speed to control flow is a new approach. In the operation of the hybrid system, the bidirectional rotational pump is driven by the electric motor so that the pump can supply pressured oil in the bi-direction. The pump sucks in oil by supplying oil from the cylinder return line and using the self-support valve to compensate for the excessive and deficient quantity of oil in the area difference of the cylinder. Because the hybrid system operates in the rotational angle and speed to satisfy the machine requirements such as pressure and flow rate, it provides energy savings and ensures lower noise generation than conventional systems. In previous research, Ahn et al. [17] studied a force control technique for the hybrid actuator where the pump is driven by an AC servo motor. The experimental results show that, although good responses were obtained even if the environment stiffness changed by for 500 [%], that system is expensive due to its use of an AC servo motor as a power supply unit. In this study, replacing the AC servo motor with a DC motor in a hybrid system reduced the price of the hybrid actuator, even though the responses of the two systems are similar. The specification of this actuator is shown in Table 1.

## 3. Comparison of energy consumption between proposed system and conventional hydraulic system

In this section, some simulations were done to compare the energy consumption between the proposed system and the conventional hydraulic system. Two hydraulic circuits representing for two methods were built in AMESim software. The schematic diagrams of both systems are shown in Fig. 3 and Fig. 4. In these simulations, the requirement for the systems

Table 1. Hybrid actuator specification.

| | | |
|---|---|---|
| 1 | Rated output | 250W |
| 2 | Rated voltage | DC24 |
| 3 | Rated flow | 0.9L/min |
| 4 | Rated pressure | 6.4MPa |
| 5 | Setting pressure of relief valve | 7.4MPa |
| 6 | Max retaining pressure | 13.7MPa |
| 7 | Cylinder rod | 20mm |
| 8 | Cylinder stroke | 300mm |

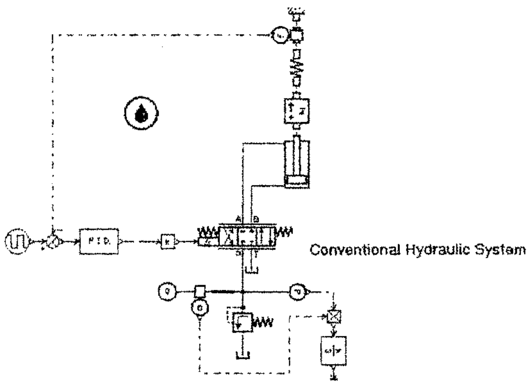


Fig. 3. Schematic diagram of a conventional hydraulic system.

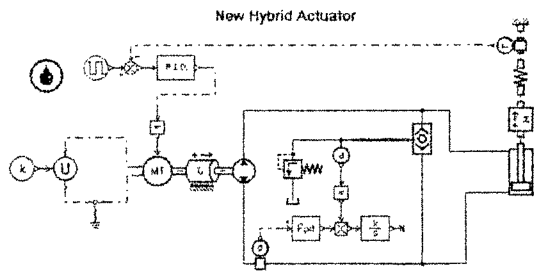


Fig. 4. Schematic diagram of the new hybrid actuator.

Table 2. Setting parameters for AMESim models.

| Parameters | | Value | Meaning |
|---|---|---|---|
| Model parameters | M (kg) | 10 | Load |
| | k (kN/m) | 10 | Environment stiffness |
| | Sensor gain (1/N) | 10 | Force sensor signal |
| | Cylinder para. (m) | 0.04x0.02x0.3 | Piston diameter x Rod diameter x Length of stroke |
| | Relief Pressure (bar) | 150 | Relief valve cracking pressure |
| Controller parameters | kP | 0.405 & 1.000 | For new hybrid actuator & conventional hydraulic system |
| | kI | 0.003 & 0.003 | |
| | kD | 0.0125 & 0.005 | |

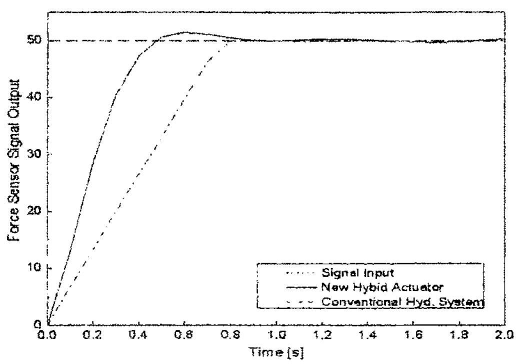


Fig. 5. Force response of hydraulics systems with PID controller.

is force control and all initial conditions are the same as shown in Table 2. Signal from force sensor connected to a load M and a spring is the feedback signal.

The first simulation is about step response. The results are shown in Fig. 5. In both hydraulic systems, PID coefficients were turned to get the best force control performance. Consequently, these values were remained for all simulations.

To prove the effectiveness of the new hybrid actuator, the simulations with the input references as step signal, sine wave and saw wave were also done. Figures from 6 to 8 are the results.

From all simulations, the energy consumptions were calculated to check the energy saving in each case by using the following equation:

$$Energy\,saving(\%) = \frac{E_{conv} - E_{new}}{E_{conv}} \times 100\% \qquad (1)$$

where $E_{conv}$ and $E_{new}$ are energy consumption of the conventional hydraulic system and the new hybrid actuator taken from the simulation outputs.

By applying Eq. 1, the energy saving for the three cases in which reference force inputs are step signal, the sine wave and saw wave are 60.71%; 55.72% and 43.01%, respectively.

From all simulation results, when comparing with the conventional hydraulic system, the energy saving features of the new hybrid actuator are clearly proved.

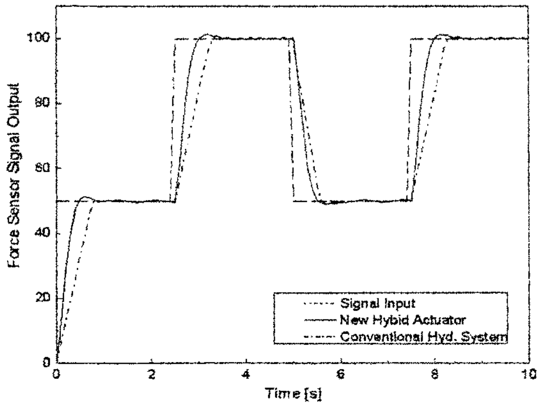


Force response

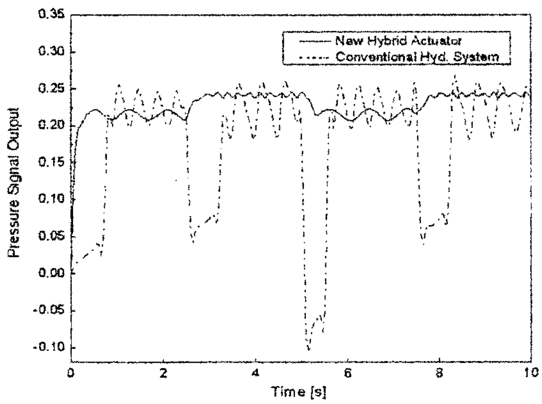


Pressure signal response

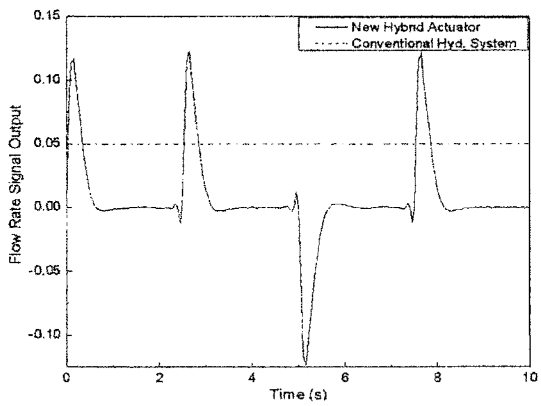


Flow rate signal response

Fig. 6. Step signal and responses of hydraulic systems.

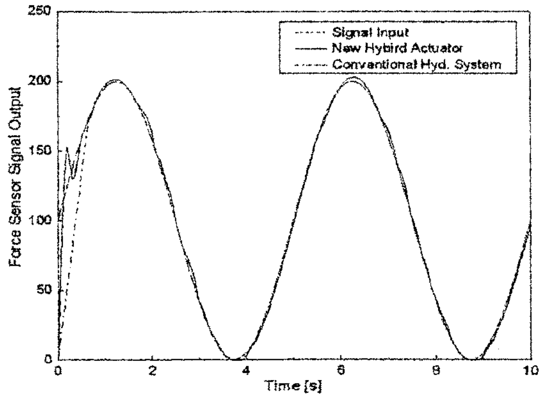


Force response

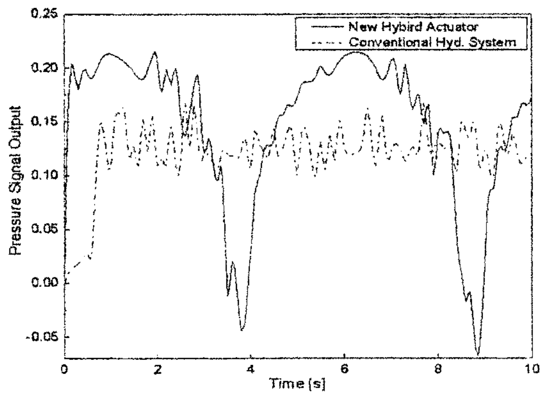


Pressure signal response

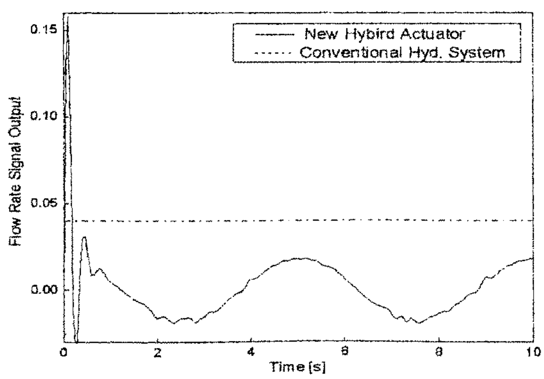


Flow rate signal response

Fig. 7. Sine wave and responses of hydraulic systems.

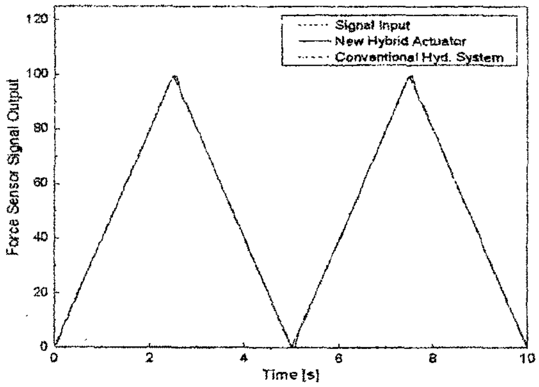


Force response

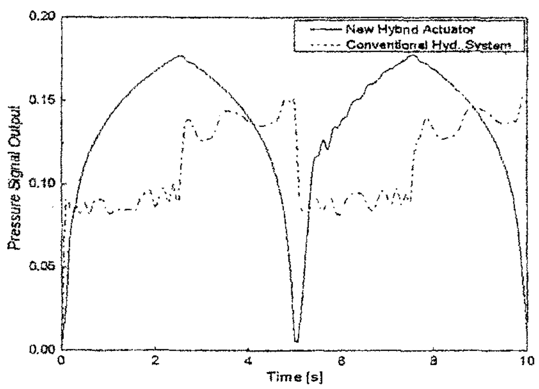


Pressure signal response

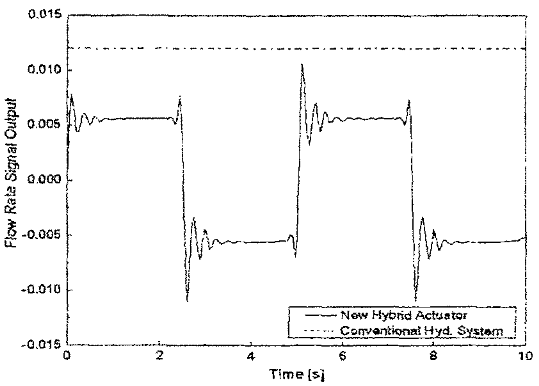


Flow rate signal response

Fig. 8. Saw wave and responses of hydraulic systems.

## 4. Robust controller design

Quantitative feedback theory (QFT) is a unified theory that emphasizes the use of feedback for achieving desired system performance tolerances despite structured plant uncertainty and plant disturbances [18]. The concept was introduced by Horowitz in the early 1960s and later refined by him and others into a controller design technique [19]. QFT is considered to be a practical engineering method for the robust controller design of continuous time feedback systems and is based on frequency-domain design methodologies. In QFT, one of the main objectives is to design a simple low-bandwidth controller that avoids problems with noise amplification, resonance frequency, and un-modeled high frequency dynamics. Fig. 9 shows the structure of a 2-DOF QFT control system in which $P(s)$ is the transfer function of the nonlinear plants (which contain parameter uncertainties), $G(s)$ is the cascade compensator, and $F(s)$ is an input filter transfer function. The output $y(t)$ is required to track the command input $r(t)$ and reject disturbances. The controller $G(s)$ is to be designed so that the variation of $y(t)$ resulting from nonlinear plant uncertainties is within allowable tolerances and that the effects of the disturbances of $y(t)$ are acceptably small. Also, the filter $F(s)$ must also be designed to achieve the desired tracking close-loop control ratio. The procedure of designing a QFT robust force controller for a hybrid actuator is described bellow.

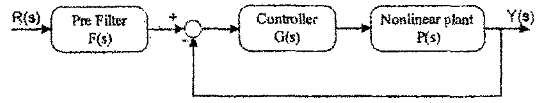


Fig. 9. Structure of the QFT control algorithm.

### *4.1 Model identification*

For the purpose of controller design, the derivation of linear time-invariant equivalent models is necessary. The first step in designing a robust QFT controller is thus to derive a family of uncertainties of the plant transfer function. An equivalent family of plants can be derived analytically, numerically from a plant model or directly from plant experimental input-output data [15]. In this study, a family of linear time invariant transfer functions for a hybrid actuator is obtained from experimental frequency responses of the system in the presence of significant uncertainty. Experimental frequency responses to a pseudo-random binary signal (PRBS) are carried out. A PRBS is randomly ordered a maximum length sequence (*m* sequence) of logic ones and zeros, emanating from a specially configured *m*-stage linear feedback shift register, which repeats after a characteristic length $L = 2^m - 1$. PRBS is deployed in the identification process with register length 8, and the bit magnitude is set to $\pm 50\ [\%]$, which corresponds to the duty cycle PWM command input. In the identification process, springs with various stiffnesses (30, 50 and 75 kN/m), represented for stiff environment were used. In each experiment, a PWM control signal generated by the PRBS was applied and the contact forces were measured at the same time. To identify a family of uncertainties of the plant transfer function, the estimation of simple process models in MATLAB [20] was used where the sampling time is 0.01s; no zeros and two real poles are set to be the system model. One sample experimental result is shown in Fig. 10. The result corresponds to the case in which the environment stiffness is 50 kN/m. As shown in the upper part of Fig. 10, the simulation and experiment result closely agree. The frequency responses of the plant are shown in Fig. 11. A hybrid actuator in contact with different environment stiffness can be presented by a family of second-order transfer functions of the following form:

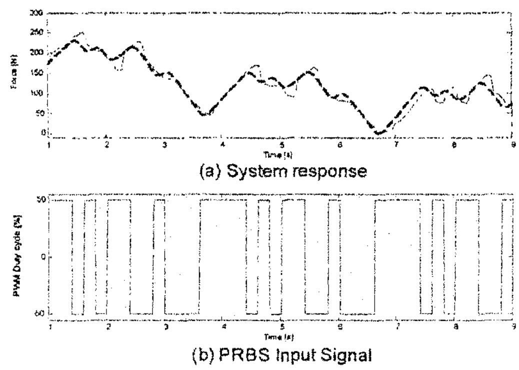


Fig. 10. Identification of the system model using PRBS.

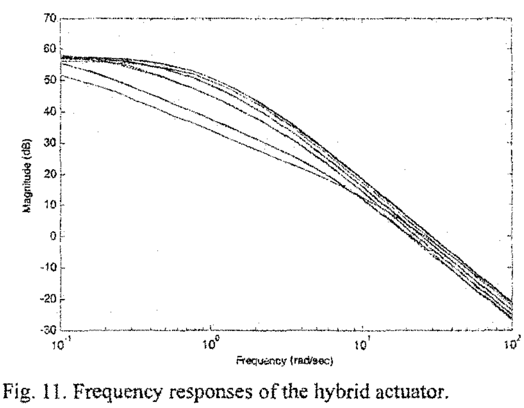


Fig. 11. Frequency responses of the hybrid actuator.

$$P_{eq}(s) = \frac{K_1}{(1+T_{p1}s)(1+T_{p2}s)}, \tag{2}$$

Here $K_1 \in [900, 1200]$; $T_{p1} \in [0.1, 0.3]$; $T_{p2} \in [3.5, 17]$;

### *4.2 QFT controller synthesis*

The objective of this section is to design a robust force controller for a hybrid actuator that is represented by the uncertainty transfer function (2). When tracking the performance requirement of system that uses QFT, it is necessary to synthesize the desired or model control ratio using the system performance's specifications in the time domain. In this system, the design specifications are set as follows to satisfy the control requirements:

- Settling time = 1.5 [s].
- Maximum percentage of overshoot $\leq 10[\%]$

The envelope of the acceptable outputs can be expressed strictly in Laplace form as follows:

$$|T_l(j\omega)| \leq |T(j\omega)| \leq |T_u(j\omega)| \quad \forall \omega \in [0, \infty) \tag{3}$$

$$\text{Where } T(s) = \frac{F(s)G(s)P(s)}{1+G(s)P(s)} \tag{4}$$

The time responses $y_u(t)$ and $y_l(t)$ in Fig. 12 represent the upper and lower bounds, respectively. For a satisfactory design, an acceptable response $y(t)$ must lie between these bounds. Fig.s 13 and 14 are the frequency plots of these bounds. The modeling of a desired transmittance $T(s)$ is discussed in detail by Horowitz [19]. After using an iteration process to find acceptable models for $T_u(s)$ and $T_l(s)$, we have

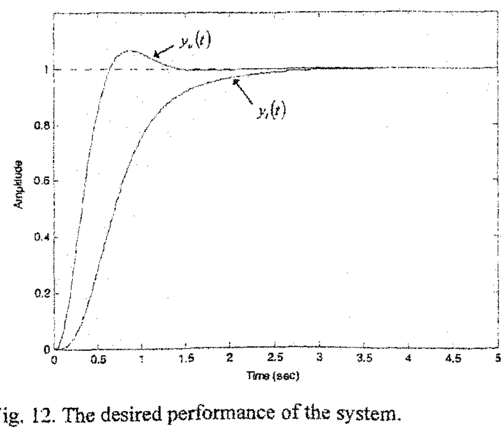


Fig. 12. The desired performance of the system.

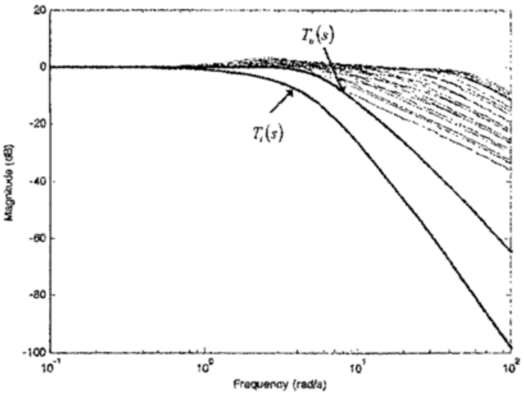


Fig. 13. Closed-loop frequency response without pre-filter.

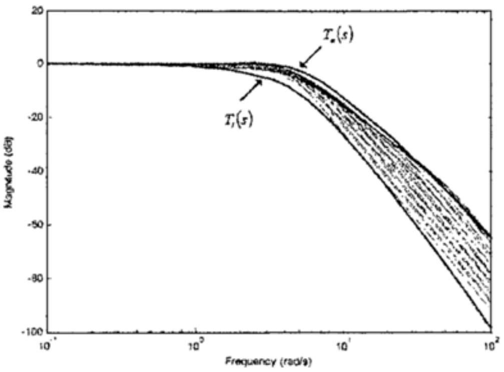


Fig. 14. Closed-loop frequency response with pre-filter.

$$T_u(s) = \frac{625}{s^3 + 31.5s^2 + 187.5s + 625}$$
$$T_l(s) = \frac{1250}{s^4 + 33.5s^3 + 250.5s^2 + 1000s + 1250} \quad (5)$$

In addition, the closed-loop *robust stability* of the closed-loop system must be checked. By the Nyquist criterion, closed-loop stability is retained as long as the loop gain does not cross the point -1 under uncertainty. In the QFT approach, *robust stability* is presented by a forbidden region about the origin which is enclosed by an *M-locus* in the Nichols chart. Hence, a gain margin for the closed-loop system of about 3 dB is given by

$$\left|\frac{L(j\omega)}{1+L(j\omega)}\right| \le M = 1.4 \quad \forall\omega \in [0,\infty) \quad (6)$$

Where $L(s)$, the closed-loop transfer function, is defined as $L(s) = P_{eq}(s)G(s)$

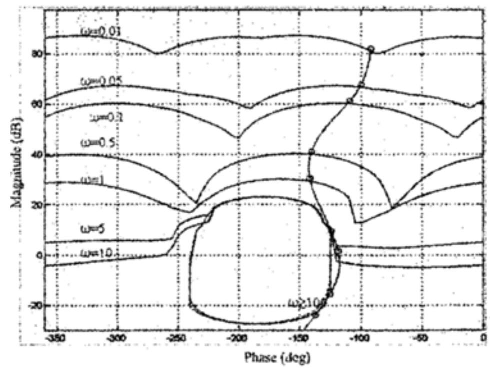


Fig. 15. QFT bounds and shaping of $L_o(j\omega)$ on the Nichols chart.

For *disturbance rejection at plant output*, the sensitive reduction problem has to be solved. Therefore, an upper tolerance is imposed on the sensitive function. Here, a constant upper bound (to limit the disturbance amplification) is used:

$$\left|S(j\omega)\right|_{\max} = \left|\frac{1}{1+L(j\omega)}\right|_{\max} \le M_D(\omega) = 1.2 \quad \forall\omega \in [0, \omega) \quad (7)$$

Eqs. (3), (6) and (7) impose constraints on nominal loop gain $|L_o(s)|$ (where $L_o(s) = P_{eo}(s)G(s)$ and $P_{eo}(s)$ denotes the nominal plant transfer function). These constraints are used to determine the tracking performance, robustness, and the output disturbance rejection boundaries on the Nichol chart at each critical frequency ($\omega$ = {0.01, 0.05, 0.1, 0.5, 1, 5, 10, 50, 100} rad/s). A feedback design satisfies these bounds if for each critical frequency the corresponding value of the loop gain is on or above the performance boundary and the output disturbance boundary and to the right or on the boundary of the robustness forbidden region. The generated QFT bounds and the final loop shaping of hybrid actuator are shown in Fig. 15. The QFT robust controller of least complexity and without overdesign is obtained by trial and error as follows:

$$G(s) = \frac{0.1367\left(\frac{s^2}{9.5481} + \frac{2.376s}{3.09} + 1\right)\left(\frac{s}{59} + 1\right)}{s\left(\frac{s}{132.6} + 1\right)\left(\frac{s}{42.38} + 1\right)} \quad (8)$$

The final step in QFT design process is the selection of the pre-filter $F(s)$. Design of a proper function

$L_e(s)$ guarantees only that the variation in $|T(j\omega)|$ is less than or equal to its constraint (3). Therefore, the purpose of the pre-filter is to position $\ln T(j\omega)$ within the frequency domain specifications. The pre-filter was found to be:

$$F(s)=\frac{0.7663s+1}{0.04521s^3+0.3459s^2+1.301s+1} \tag{9}$$

The effect of the pre-filter is illustrated by comparing closed-loop frequency response both with and without a pre-filter. From Fig.s 13 and 14, it is clear that all tracking specifications are satisfied in frequency domain.

## 5. Experimental results

In this section, experiments were conducted to show the effectiveness of the designed robust controller. To investigate the tracking performance and robustness of the QFT controller, the contact environment was changed from a low stiffness (30 kN/m) to a high one (75 kN/m). First, a conventional PID controller was applied; Figs. 16 and 17 give the force response results with different environments stiffness (30 and 75 kN/m, respectively), where the control gains are fixed as the maximum and minimum environment stiffness, respectively. In addition, the response to various set-point forces is shown in Fig. 18. These results show that the system responses become more oscillatory and exhibit more overshoot at lower environmental stiffnesses. Moreover, the responses become slower and less stable if the set-point force is changed. Hence, the robust force controller described by transfer function (8) is implemented to overcome these control problems. The robust experimental results (for an environmental stiffness of 75 kN/m) are shown in Fig. 19. A comparison of system responses using a conventional PID controller and a QFT robust controller is given in Fig. 20 (using a stiffness of 30 kN/m). The tracking ladder signal force set-point is investigated to compare the results for different set-point forces (Fig. 21, 22 and 23). The experimental results clearly show that a good force regulation is realized in the case of using a QFT technique to design a robust force controller. Moreover, the designed controller is capable of handling the variations in environmental stiffness, the steady state errors are small (about 1%), and the system can be adapted with various set-point forces.

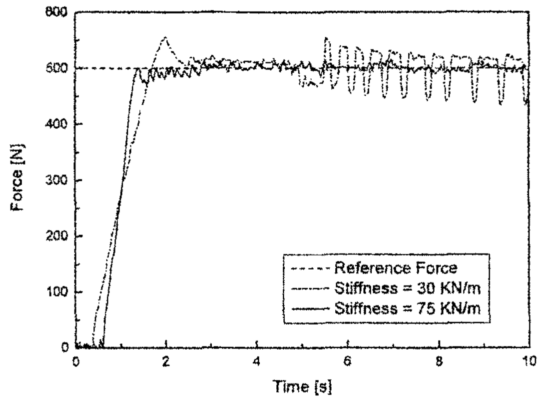


Fig. 16. Force response of hybrid actuator with conventional PID controller ($K_P$ = 0.06; $K_I$ = 0.008; $K_D$ = 0.0005, turned for 75 kN/m).

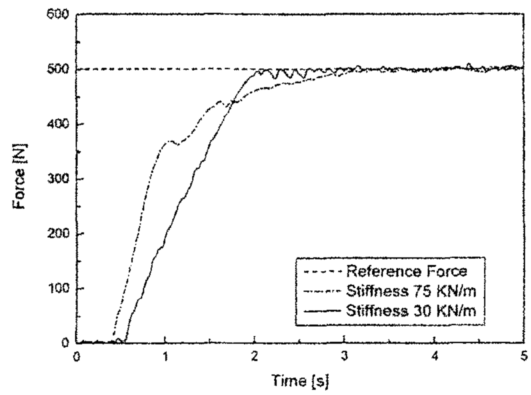


Fig. 17. Force response of hybrid actuator with conventional PID controller ($K_P$ = 0.078; $K_I$ = 0.012; $K_D$ = 0.0003, turned for 30 kN/m).

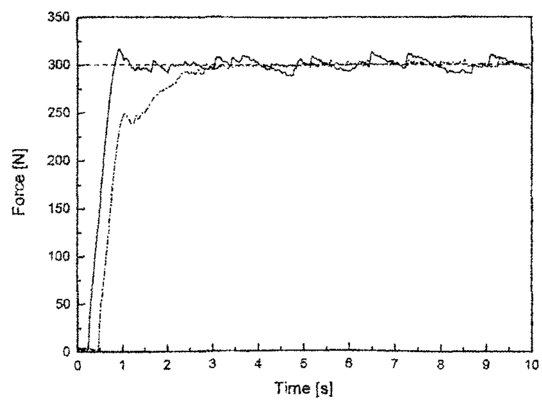


Fig. 18. Force response of hybrid actuator with conventional PID controller ($K_P$ = 0.06; $K_I$ = 0.008; $K_D$ = 0.0005, turned for 500 N reference force).

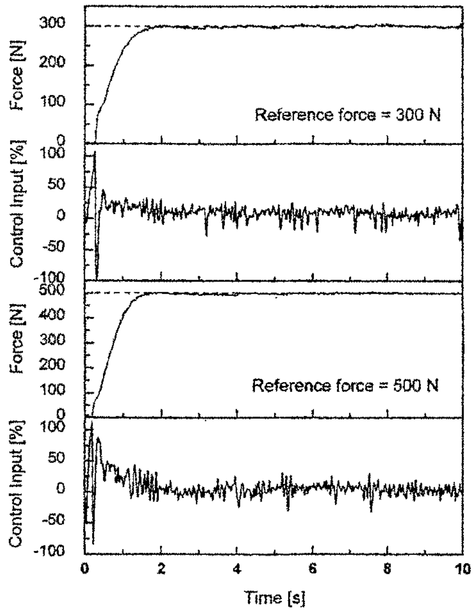


Fig. 19. Force response with QFT controller when the stiffness is 75 kN/m.

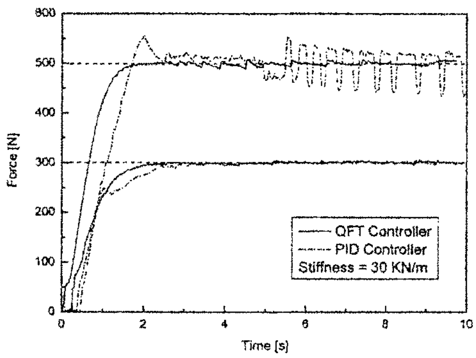


Fig. 20. Comparison of system responses in conventional PID controller and QFT robust controller when the stiffness is 30 kN/m.

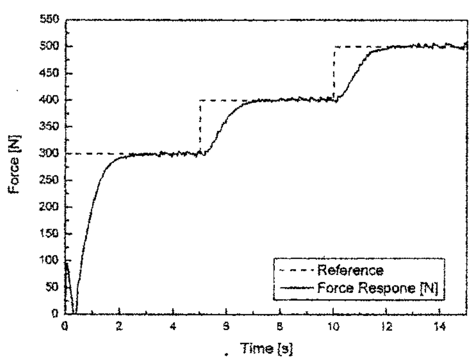


Fig. 21. Force response to ladder signal force set-point when the stiffness is 75 kN/m.

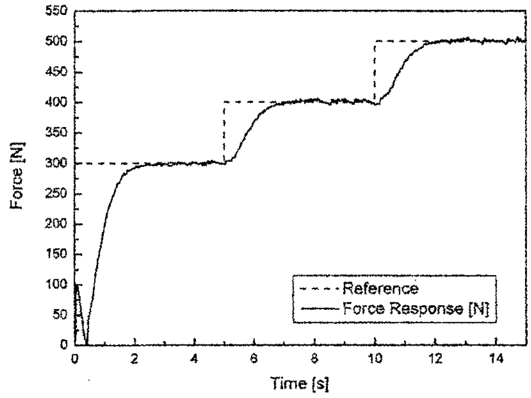


Fig. 22. Force response to ladder signal force set-point when the stiffness is 50 kN/m.

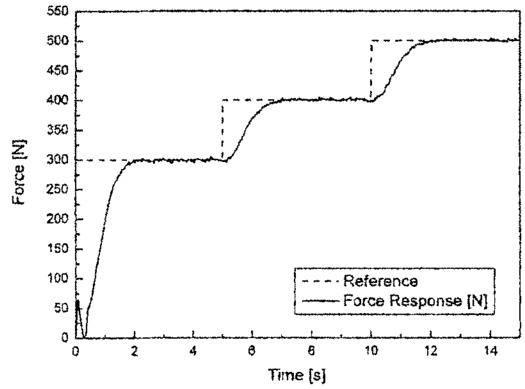


Fig. 23. Force response to ladder signal force set-point when the stiffness is 30 kN/m.

## 6. Conclusions

This paper presents a systematic approach to the design and experimental evaluation of a robust force control of a new energy-saving hybrid actuator by using the QFT design technique. A family of plant models for a hybrid actuator is obtained experimentally from the frequency responses by using PRBS as control signal in the presence of significant uncertainty. Several experiments were performed under variation of up to 250% in environmental stiffness (from 30 kN/m to 75 kN/m). The experimental results demonstrated convincingly that the robust force controller designed by QFT methodology can satisfy the robust performance requirements, tracking performance specifications, and disturbance attenuation requirements.

The second contribution of this paper is the introduction of a new low-cost hybrid actuator using DC motor as a power supply unit. Moreover, the control methodology presented here can be applied to automation, such as the end-effector of a robot system, plastic injection-molding, metal forming technology and hydraulic excavator machines.

## Acknowledgments

This work was supported by the Korea Research Foundation Grant Funded by the Korea Government (MOEHRD) (KRF-2005-211-D00018).

## References

[1] R. Rahmfeld and M. Ivantysynova, Displacement controlled linear actuator with differential cylinder - a way to save primary energy in mobile machines, In Proc. of the 5th Int. Conf. on Fluid Power Transmission and Control (ICFP), Hangzhou, China. (2001) 316-322.

[2] J. Andersson, P. Krus and K. Nilsson, Optimization as a support for selection and design of aircraft actuation systems, In Proc. of the Seventh AIAA/USAF/NASA/ISSMO Symposium on Multidisciplinary Analysis and Optimization, St. Louis, USA. (1998).

[3] B. Yao, F. Bu, J. Reedy and G. Chiu, Adaptive robust motion control of single-rod hydraulic actuators: theory and experiments, In IEEE/ASME Trans. on Mechatronics. 5 (1) (2000) 79-91.

[4] A. Alleyne, R. Liu and H. Wright, On the limitation of force tracking control for hydraulic active suspensions, In Proc. of the American Control Conf. (1998) 43-47.

[5] Y. N. Chen, B. C. Lee and C. H. A. Tseng, Variable-structure controller design for an electro-hydraulic force control servo system, *J. Chin. Soc. Mech. Engrs.* 11 (6) (1990) 520-526.

[6] G. Wu, N. Sepehri and K. Ziaei, Design of a hydraulic force motion control system using a generalized predictive control algorithm, In IEE Proc. on Control Theory and Applications. 145 (5) (1998) 428-436.

[7] F. Conrad and C. J. D. Jensen, Design of hydraulic force control systems with state estimate feedback, In Proc. of the IFAC 10th Triennial Congress, Munich, Germany. (1987) 307-312.

[8] J. Grabbel, On the control of joint integrated servo actuators for mobile handling and robotic applications, In Proc. of the 1st FPNI-PhD Symp. Hamburg. (2000) 449-465.

[9] J. Andersson, Sensitivity analysis in Pareto optimal design, In Proc. of the 4th Asia-Pacific Conf. on Simulated Evolution and Learning, SEAL 02, Singapore. (2002) 18-22.

[10] J. Andersson, P. Krus, K. Nilsson and K. Storck, Modelling and simulation of heat generation in electro-hydrostatic actuation systems, In Proc. of the 4th JHPS Int. Symposium on Fluid Power, Tokyo, Japan. (1999) 15-17.

[11] J. Andersson, P. Krus and D. Wallace, Multiobjective optimization of hydraulic actuation systems, In Proc. of ASME Design Automation Conf., Baltimore, USA. (2000) 11-13.

[12] M. B. Leahy, D. E. Bossert and P. V. Whalen, Model-based control with quantitative feedback theory, In Proc. of IEEE Int. Conf on Robotics and Automation, (1) (1990) 1982-1987.

[13] D. Thompson, J. S. Pruyn and A. Shukla, Feedback design for robust tracking and robust stiffness in flight control actuators using modified QFT technique, In Proc. of ACC Conf., San Diego, CA, USA. (1999) 754-758.

[14] S. J. Rober, Y. C. Shin and O. D. I. Nwokah, A digital robust controller for cutting force control in the end milling process, *ASME journal of Dynamic System, Measurement and Control.* 119 (2) (1997) 146-152.

[15] N. Niksefat and N. Sepehri, Robust force controller design for a hydraulic actuator based on experimental input-output data, In Proc. of the American Control Conf. 5 (5) (1999) 3718-3722.

[16] D. F. Thompson and G. G. Kremer, Quantitative feedback design for a variable-displacement hydraulic vane pump, In Proc. of the American Control Conf. 2 (2) (1997) 1061-1065.

[17] K. K. Ahn and H. T. C. Nguyen, Force control of hybrid actuator using learning vector quantization neural network, *In KSME Int. Journal of Mechanical Science and Technology.* 20 (4) (2006) 447-454.

[18] J. J. D'Azzo and C. H. Houpis, Linear Control System Analysis and Design, McGraw-Hill, New York, USA, (1998).

[19] I. M. Horowitz, Quantitative Feedback Design Theory (QFT), CO: QFT, Boulder, (1992).

[20] L. Lennart, System Identification Toolbox – for use with MATLAB, The Mathworks Inc., Natick, Massachusetts, (1995).